Fano Resonance Resulting from a Tunable Interaction between Molecular Vibrational Modes and a Double Continuum of a Plasmonic Metamolecule

E. J. Osley,[1,2] C. G. Biris,[2] P. G. Thompson,[1,2] R. R. F. Jahromi,[1,2] P. A. Warburton,[1,2] and N. C. Panoiu[2,3]

[1]*London Centre for Nanotechnology, University College London, 17-19 Gordon Street, London WC1H 0AH, United Kingdom*

[2]*Department of Electronic and Electrical Engineering, University College London, Torrington Place, London WC1E 7JE, United Kingdom*

[3]*Thomas Young Centre, London Centre for Nanotechnology, University College London, 17-19 Gordon Street, London, WC1H 0AH, United Kingdom*

(Received 15 August 2012; revised manuscript received 12 November 2012; published 19 February 2013)

Coupling between tunable broadband modes of an array of plasmonic metamolecules and a vibrational mode of carbonyl bond of poly(methyl methacrylate) is shown experimentally to produce a Fano resonance, which can be tuned *in situ* by varying the polarization of incident light. The interaction between the plasmon modes and the molecular resonance is investigated using both rigorous electromagnetic calculations and a quantum mechanical model describing the quantum interference between a discrete state and two continua. The predictions of the quantum mechanical model are in good agreement with the experimental data and provide an intuitive interpretation, at the quantum level, of the plasmon-molecule coupling.

DOI: 10.1103/PhysRevLett.110.087402 PACS numbers: 78.67.Pt, 42.82.Et, 73.20.Mf, 78.68.+m

The spectral control of optical absorption in metallic nanostructures has generated much interest, both as a means for studying light-matter interaction at the deep-subwavelength scale and to develop new functional nanomaterials. Plasmonic materials provide an ideal platform for achieving enhanced optical interaction at the nanoscale as their primary building blocks consist of highly resonant particles, which strongly confine and enhance the optical field [1–4]. These properties are commonly employed to increase the optical coupling between plasmonic structures and an optically active medium, enabling many applications, including surface-enhanced Raman [5,6] and infrared absorption [7,8] spectroscopies, enhancement of the excitation rate and fluorescence of quantum dots and molecules [9–11], chemical sensing [12,13], and biodetection [14,15]. One effective approach for tailoring the shape of plasmonic resonances is the Fano interference between a narrow (discrete) resonance and a broad (continuous) one [16–19].

A defining feature of Fano resonances is their pronounced spectral asymmetry. This can be exploited in applications that require high sensitivity to changes in the environment. Fano resonances in plasmonic systems can also provide physical insights into light-matter interaction at the nanoscale, as they are primarily the result of short-range, near-field interactions. Although Fano resonances in plasmonic systems have been chiefly investigated in a classical context, they can also be observed in quantum systems consisting of quantum dots, atoms, or molecules coupled to metallic nanoparticles [14,20–22]. In this case the Fano resonance results from the interaction between a quantum discrete state and a classical continuum (localized or extended) plasmon mode. In many applications it is desirable to tune the strength of the interaction between the discrete and continuous state, and consequently dynamically change the shape of Fano resonances. However, since the materials and geometrical parameters of a plasmonic structure are difficult to control at the nanoscale, a convenient way to achieve optical tunability has not yet been attained.

In this Letter we demonstrate experimentally and theoretically an efficient approach to achieve *in situ* tuning of the strength of the interaction between optically active vibrational modes of molecules—here the carbonyl bond of poly(methyl methacrylate) (PMMA)—and the localized surface plasmon (LSP) modes of plasmonic metamolecules consisting of asymmetric cross apertures in a thin metallic film (see Fig. 1). These nanostructures have been studied extensively [23,24], one of their defining properties being that, analogous to anisotropic molecules, their polarizability strongly depends on the polarization of the incident wave. These metamolecules can thus be tailored to different molecular resonances not only because the resonance frequencies of LSPs are strongly dependent upon their size and shape but, more importantly, because of their intrinsic optical anisotropy.

Sample fabrication.—A 1 mm thick CaF_2 substrate was partially coated with a 5 nm chromium adhesion layer and a 35 nm gold film by thermal evaporation. The array shown in Figs. 1(a) and 1(b) was patterned using electron-beam lithography and argon-ion milling. The aperture geometry, and the orientation of the electric field, **E**, of incident polarized light relative to the apertures is shown in Fig. 1(c). The apertures have arm lengths $L_x = 1900$ nm and $L_y = 1340$ nm and widths $G_x = 580$ nm and $G_y = 360$ nm. The surface was spin coated with a 85 nm PMMA

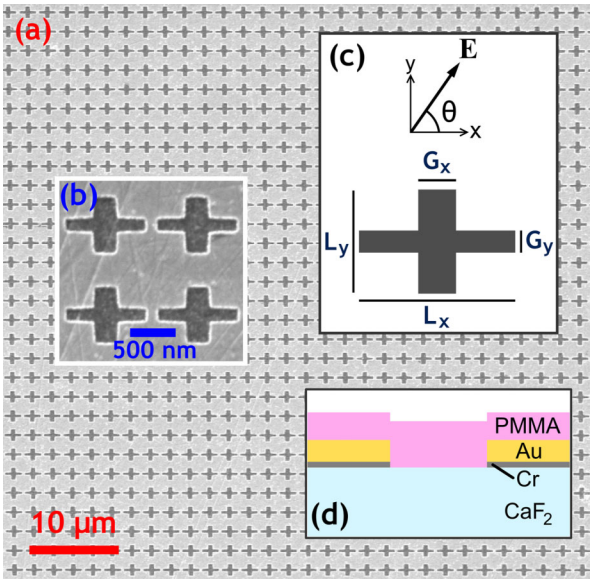

FIG. 1 (color online). (a) Scanning-electron micrograph showing part of the cruciform aperture array before PMMA coating. (b) Magnified detail of four apertures. (c) Aperture geometry showing the in-plane electric field polarization angle, θ. (d) Schematic cross section of the structure following PMMA coating.

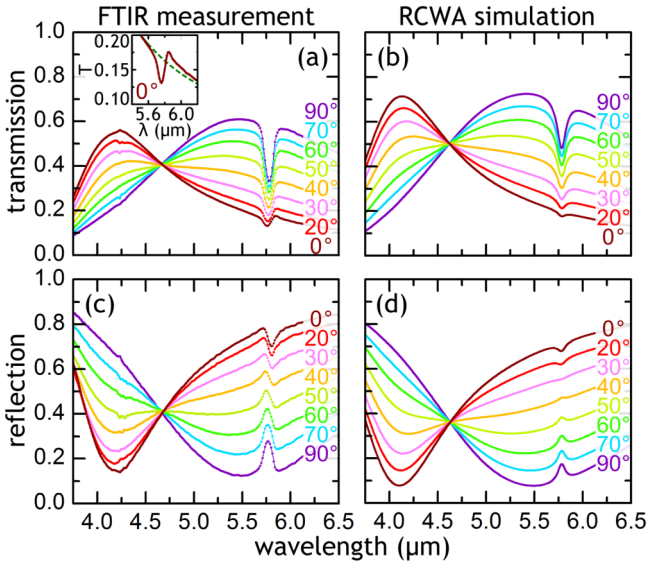

FIG. 2 (color online). (a) Transmission and (c) reflection of the structure measured using FTIR; (b) transmission and (d) reflection simulated using the RCWA method. The incident polarization angle θ varies from zero (brown) to $\theta = 90°$ (purple). The resonance of the PMMA carbonyl bond is visible at $\lambda = 5.79$ μm. The inset to (a) shows the measured spectrum (solid line) and the fitted base line (broken line) at the carbonyl bond resonance for $\theta = 0°$.

film, filling the apertures. Figure 1(d) shows the final structure in cross section.

Optical characterization.—The transmission and reflection spectra of the array were measured using Fourier transform infrared spectroscopy (FTIR) microscopy. The source is a broadband mid-IR globar which is focused onto the sample. The light is collimated and passed through an aperture which selects radiation being transmitted or reflected from a circular sample area 79 μm in diameter. The signal was detected using a HgCdTe detector. The reflection spectra R and transmission spectra T of the samples were normalized to spectra obtained from uncoated areas of gold film and CaF_2 substrate, respectively. The incident radiation was linearly polarized using a wire grid polarizer with an extinction ratio of 168:1 at 5 μm. Figures 2(a) and 2(c) show, respectively, the measured transmission and reflection spectra of the aperture array coated with PMMA. In the transmission spectra two global maxima are present: one, at 4.2 μm occurs when the polarization angle $\theta = 0$ and another, at 5.5 μm, when $\theta = 90°$. These global maxima are due to the excitation of two LSP modes, which are supported by the apertures [23,24]. In the reflection spectra the excitation of the plasmon modes produces global minima. Spectral kinks at 4.23 μm, caused by atmospheric CO_2 variation between the sample and normalization spectra, are neglected in our analysis. The spectral signature of the PMMA carbonyl bond is located at 5.79 μm. The shape of the carbonyl resonance peak changes with θ, showing a more pronounced, asymmetric Fano-like line shape as θ approaches zero. The interaction of the two broad plasmon resonances with the narrow molecular resonance forms the Fano resonance at 5.79 μm. The inset to Fig. 2(a) also shows that, for small values of θ, at wavelengths somewhat longer than the carbonyl bond resonant wavelength, the transmission can be larger than the baseline value in spite of the fact that PMMA is a lossy dielectric. This is an example of absorption-induced transparency [25]. Furthermore, as shown in Fig. 2(c) the reflectivity of the aperture array decreases with respect to the baseline for small θ, whereas it increases for large θ, by as much as $\sim$100% for $\theta = 90°$. This phenomenon we refer to as absorption-induced reflectivity.

Numerical simulations.—To model the optical response of our PMMA-coated device we used commercially available software [26] based on the rigorous coupled wave analysis (RCWA). We used a constant refractive index for the CaF_2 substrate, a Lorentz-Drude model for the Au and Cr layers [27], and a complex refractive index for the PMMA layer (found by fitting the numerically determined transmission to an experimental measurement of the transmission of a 85 nm thick PMMA film). Figures 2(b) and 2(d) show the transmission and reflection spectra, respectively, found by numerical simulations; the experimental data show slightly less transmission and more reflection because sample nonuniformity, e.g., surface roughness, is not included in the model. The simulations also allow spatial field profiles to be calculated; Fig. 3 shows the spatial profile of the field enhancement

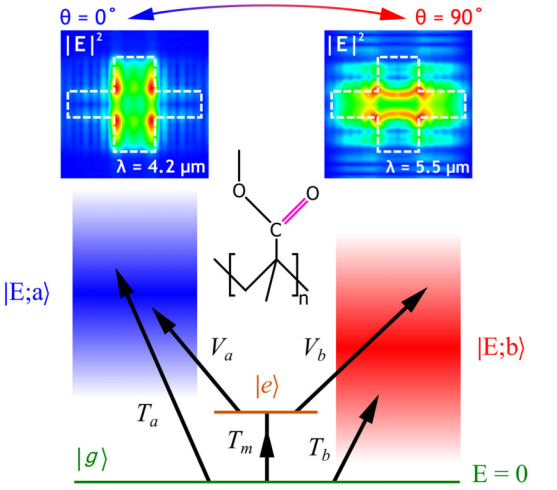

FIG. 3 (color online). System schematic showing the ground state $|g\rangle$, the two LSP continua, $|E;a\rangle$ and $|E;b\rangle$, and the discrete molecular resonance $|e\rangle$. Simulated spatial profiles (taken in the x-y plane at the center of the aperture) show large field enhancement for $\theta = 0$ at $\lambda = 4.2$ μm and $\theta = 90°$ at $\lambda = 5.5$ μm. Aperture boundaries are indicated by dashed lines. The atomic structure of the PMMA monomer is shown; the resonance of the carbonyl (C═O) bond corresponds to the excited state $|e\rangle$.

corresponding to the two LSPs. For measurements and simulations of an uncoated aperture array see the Supplemental Material [28].

Theoretical model for molecule-plasmon metamolecule interaction.—In what follows we introduce a simple quantum mechanical model describing the interaction between the molecular vibrational mode and the LSP resonances. Figure 3 shows the interacting quantum mechanical system schematically.

We assume that the interacting system is described by a Hamiltonian, $\hat{H} = \hat{H}_0 + \hat{V}_a + \hat{V}_b$, where $\hat{H}_0 = \hat{H}_m + \hat{H}_a + \hat{H}_b$ is the Hamiltonian of the noninteracting molecule ($\hat{H}_m$) and the two LSPs ($\hat{H}_a$ and $\hat{H}_b$) and $\hat{V}_a$ and $\hat{V}_b$ describe the interaction between the molecule and the two LSPs. The molecule is modeled as a two-level system with $|g\rangle$ and $|e\rangle$ the ground and excited states, respectively. We assume that the eigenstates corresponding to the energy E, $|E;a\rangle$ ($|E;b\rangle$), of $\hat{H}_a$ ($\hat{H}_b$) form two continua. Note that the two plasmon modes are orthogonal and thus the continua are orthogonal, too: $\langle E;a|E';b\rangle = \delta_{ab}\delta(E - E')$.

Under these conditions we can write $\hat{H}_0$ as

$$\hat{H}_0 = E_g|g\rangle\langle g| + E_e|e\rangle\langle e| + \sum_{i=a,b}\int E|E;i\rangle\langle E;i|dE, \quad (1)$$

where E_g and E_e are the energies of the ground and excited state of the molecule, respectively. The interaction between the molecule and the two LSPs (continua) can be expressed as $\hat{V}_i = \int V_{i,E}|E;i\rangle\langle e|dE + \text{H.c.}$, $i = a, b$, where $V_{i,E} = \langle E;i|\hat{V}_i|e\rangle$, $i = a, b$, are the matrix elements of $\hat{V}_i$ and are proportional to the local electric field of the LSP and H.c. means Hermitian conjugate. Introducing the density of states of the two continua, $\rho_{a,b}(E)$, these matrix elements are written as $V_{i,E} = v_i\sqrt{\rho_i(E)}$, $i = a, b$. We assume that the spectra of the plasmon A (B) is described by a Lorentzian centered at the plasmon energy E_a (E_b) with width Γ_a (Γ_b),

$$\rho_i(E) = \frac{1}{1 + [\frac{2(E-E_i)}{\Gamma_i}]^2}, \qquad i = a, b. \quad (2)$$

Following the approach of Fano [16], the total Hamiltonian $\hat{H}$ can be orthogonalized in a new basis of eigenstates which form two orthogonal continua, i.e., $\langle E;1|\hat{H}|E';1\rangle = \langle E;2|\hat{H}|E';2\rangle = E\delta(E - E')$, where $\langle E;1|E';2\rangle = 0$. These eigenstates can be written as [16]

$$|E;1\rangle = \frac{\sin\Delta}{\sqrt{\pi\gamma}}|\Phi_E\rangle - \cos\Delta|\tilde{\psi}_E\rangle; |E;2\rangle = |\tilde{\psi}_E\rangle, \quad (3)$$

where $|\Phi_E\rangle$ is the "dressed" excited state $|e\rangle$ modified by the interaction with the two continua,

$$|\Phi_E\rangle = |e\rangle + \sum_{i=a,b}\fint dE'\frac{V_{i,E'}}{\sqrt{\pi\gamma(E')}(E - E')}|E';i\rangle, \quad (4)$$

(here $\fint$ means the Cauchy principal value of the integral) and $|\bar{\psi}_E\rangle$ and $|\tilde{\psi}_E\rangle$ are two continuum states defined as:

$$|\bar{\psi}_E\rangle = \sqrt{\pi/\gamma(E)}(V_{a,E}|E;a\rangle + V_{b,E}|E;b\rangle), \quad (5a)$$

$$|\tilde{\psi}_E\rangle = \sqrt{\pi/\gamma(E)}(V^*_{b,E}|E;a\rangle + V^*_{a,E}|E;b\rangle). \quad (5b)$$

In Eq. (3) Δ determines the phase shift induced by quantum interference between the discrete state $|e\rangle$ and the two continua, and γ describes the width of the modified excited state. They are given by

$$\gamma(E) = \pi(|V_{a,E}|^2 + |V_{b,E}|^2) \equiv \frac{\Gamma_m}{2}, \quad (6a)$$

$$\Delta(E) = -\arctan\frac{\gamma(E)}{E - E_e - \Sigma(E)}, \quad (6b)$$

where the energy shift of the excited state is

$$\Sigma(E) = \fint\frac{\gamma(E')}{\pi(E - E')}dE'. \quad (7)$$

The interaction between the coupled molecule-metamolecule system and a plane wave normally incident onto the array can be described by a Hamiltonian $\hat{T} = \hat{T}_m + \hat{T}_a + \hat{T}_b$, with $\hat{T} = t_{e0}|e\rangle\langle 0| + \sum_{i=a,b}\int T_{i,E}|E;i\rangle\times\langle 0|dE + \text{H.c.}$ Here, $|0\rangle$ is the ground state of the interacting system, in which the molecule is in the ground state and no plasmons are excited. The matrix elements of T are: $t_{e0} = \langle e|\hat{T}_m|0\rangle$, $T_{a,E} = \langle E;a|\hat{T}_a|0\rangle \equiv \mu_a\sqrt{\rho_a(E)}\cos\theta$, and $T_{b,E} = \langle E;b|\hat{T}_b|0\rangle \equiv \mu_b\sqrt{\rho_b(E)}\sin\theta$, where $\mu_{a,b}$ quantify the coupling strength between the incoming plane

wave and the two LSPs, and we have used the fact that the plasmon A (B) is excited by a $y(x)$-polarized wave.

Using Fermi's golden rule, the rate at which the system absorbs photons of frequency ω is $\mathcal{W}(\omega) = \frac{2\pi}{\hbar}\sum_{i=1,2}\int dE|\langle E; i|\hat{T}|0\rangle|^2\delta(\hbar\omega - E)$. Inserting Eqs. (3) in this equation one obtains the absorption of the system,

$$A(\omega) = \mathcal{N}\omega[|\langle\bar{\psi}_{\hbar\omega}|\hat{T}|0\rangle|^2 F(q,\epsilon) + |\langle\tilde{\psi}_{\hbar\omega}|\hat{T}|0\rangle|^2], \quad (8)$$

where $\mathcal{N} = 2\pi n_s/I_0$ is a constant, with n_s, and I_0 being the number of molecules per area and the intensity of the incoming beam, respectively, and $F(q,\epsilon) = (q+\epsilon)^2/(\epsilon^2+1)$ is the Fano function. The asymmetry parameter, q, and the reduced energy, ϵ, are given by

$$q = \frac{\langle\Phi_{\hbar\omega}|\hat{T}|0\rangle}{\sqrt{\pi\gamma(\hbar\omega)}\langle\bar{\psi}_{\hbar\omega}|\hat{T}|0\rangle}; \qquad \epsilon = \frac{\hbar\omega - E_e - \Sigma(\hbar\omega)}{\gamma(\hbar\omega)}. \quad (9)$$

The absorption spectrum in Eq. (8) shows that the coupling of the molecular vibrational mode with the two continua of the plasmonic metamolecule leads to a resonant response of the optical system around the energy of the vibrational mode, $\hbar\omega \simeq E_e$, which is superimposed on a broad background. Hence, unlike the case of only one continuum, the absorption does not cancel at the frequency for which $F(q,\epsilon) = 0$, i.e., when $q = -\epsilon$.

The interaction between the incoming light and the plasmons can be tuned by varying the polarization angle; this allows one to modify the mixture of the two LSPs and, consequently, one can easily tune the strength of the interaction between the vibrational mode and the plasmonic metamolecule. In order to provide a more quantitative description we assume that the normalized densities of state of the two LSPs are given by Eq. (2). Then, the matrix elements in Eq. (8) and the parameters of the Fano function can be calculated explicitly. The absorption can be cast as

$$A(\omega) = \frac{\mathcal{N}\pi\omega}{\gamma(\hbar\omega)}[|\mu_a v_a^*\rho_a\cos\theta + \mu_b v_b^*\rho_b\sin\theta|^2 F(q,\epsilon) + \rho_a\rho_b|\mu_a v_b\cos\theta + \mu_b v_a\sin\theta|^2], \quad (10)$$

where the Fano parameters are

$$q = 2\frac{\frac{t_{e0}}{2\pi} + \frac{\hbar\omega - E_a}{\Gamma_a}\mu_a v_a^*\rho_a\cos\theta + \frac{\hbar\omega - E_b}{\Gamma_b}\mu_b v_b^*\rho_b\sin\theta}{\mu_a v_a^*\rho_a\cos\theta + \mu_b v_b^*\rho_b\sin\theta}, \quad (11a)$$

$$\epsilon = \frac{2}{\Gamma_m}\left[\hbar\omega - E_e - \pi\left(\rho_a|v_a|^2\frac{\hbar\omega - E_a}{\Gamma_a} + \rho_b|v_b|^2\frac{\hbar\omega - E_b}{\Gamma_b}\right)\right]. \quad (11b)$$

Comparison between theory and experiment.—To fit the model to the experimental system the absorption $A = 1 - T - R$ of the structure was extracted from the measured transmission and reflection data, as shown in Fig. 4(a). From this the parameters $E_{a,b}$ and $\Gamma_{a,b}$ can be directly extracted; E_a and Γ_a from the $\theta = 0$ data and E_b and Γ_b from the $\theta = 90°$ data. E_e and Γ_m (the carbonyl bond parameters) are taken from transmission measurements of a 100 nm PMMA film. The parameters $v_{a,b}$, $\mu_{a,b}$, and t_{e0} are then extracted for each value of θ using an unconstrained least squares method (for a list of symbols and their fitted values, see the Supplemental Material [28]).

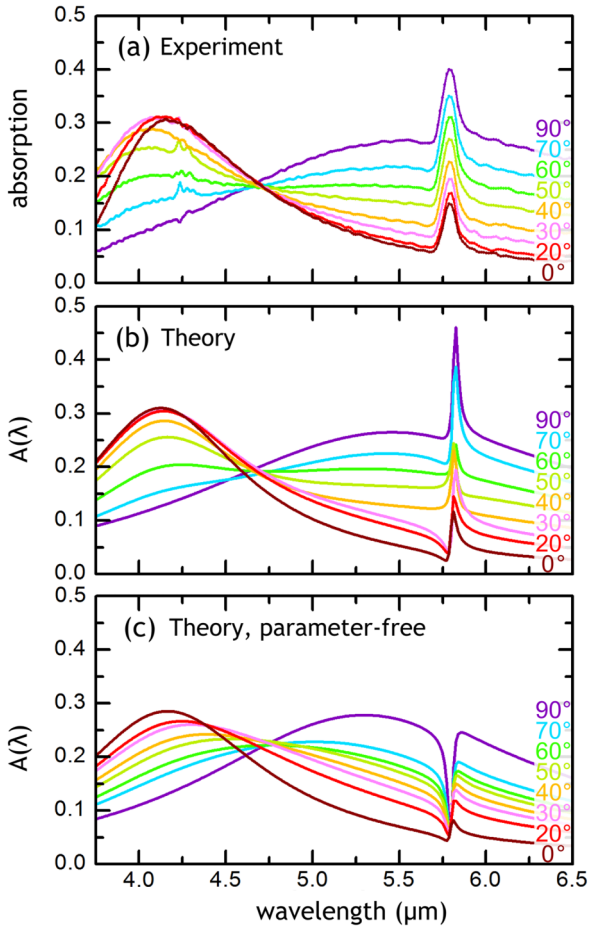

FIG. 4 (color online). (a) Absorption of the structure, from FTIR measurements of transmission and reflection. (b) Best fit of experimental data using Eq. (10). (c) Parameter-free modeling of the system.

Figure 4(b) shows the predictions of the model following fitting. There is good agreement between the measured spectra and those predicted by the model at all values of θ. In particular, all the main features of the Fano resonance are reproduced by our theoretical model, e.g., the increase of the optical absorption as θ is varied from zero to 90°. Our model also predicts that $t_{e0} \ll |v_{a,b}|^2$ for all angles θ, which means that, as expected, the molecules interact primarily with the optical near field of the LSPs. This proves that our model can be used to gain insights into the interaction between quantum and plasmonic systems as it allows one to retrieve the values of basic quantities, e.g., $v_{a,b}$, $\mu_{a,b}$, and t_{e0}, which characterize these interactions at

the nanoscale. Figure 4(c) shows the predictions of the model if the fitted parameters are estimated using a parameter-free approach, i.e., $|\mu_{a,b}|^2 = \Gamma_{a,b}/2\pi$ and $|v_a|^2 = |v_b|^2 = \Gamma_m/2\pi \equiv t_{e0}$ [22]. The poor agreement with experimental data occurs because the coupling coefficients $v_{a,b}$ depend on the spatial distribution of the optical near field and thus one cannot assume that they are the same for all LSPs.

In conclusion, we have demonstrated that plasmonic structures allow *in situ* tuning of the optical coupling between a quantum and a classical system by selecting the polarization of incident light. This tuning produces a change in the spectral line shape about the optical resonance of the quantum system, a consequence of the Fano resonance produced by the coupling of broad and narrow resonances. The system has been described using an intuitive quantum mechanical model, which allows a deeper understanding of the underlying physics. Our study has the potential to foster exciting new developments in subwavelength optics and nanophotonics and in the emerging field of quantum plasmonics. Equally important, the system investigated here has the potential to improve the range and versatility of a series of nanodevices, including chemical and biological plasmonic sensors.

This work was supported by EPSRC.

[1] W. L. Barnes, A. Dereux, and T. W. Ebbesen, Nature (London) **424**, 824 (2003).
[2] A. V. Zayats, I. I. Smolyaninov, and A. A. Maradulin, Phys. Rep. **408**, 131 (2005).
[3] F. Garcia-Vidal, L. Martin-Moreno, T. Ebbesen, and L. Kuipers, Rev. Mod. Phys. **82**, 729 (2010).
[4] S. A. Maier, *Plasmonics: Fundamentals and Applications* (Springer, New York, 2007).
[5] S. M. Nie and S. R. Emery, Science **275**, 1102 (1997).
[6] K. Kneipp, Y. Wang, H. Kneipp, L. T. Perelman, I. Itzkan, R. R. Dasari, and M. S. Feld, Phys. Rev. Lett. **78**, 1667 (1997).
[7] D. Enders and A. Pucci, Appl. Phys. Lett. **88**, 184104 (2006).
[8] J. Kundu, F. Le, P. Nordlander, and N. J. Halas, Chem. Phys. Lett. **452**, 115 (2008).
[9] J. H. Song, T. Atay, S. Shi, H. Urabe, and A. Nurmikko, Nano Lett. **5**, 1557 (2005).
[10] P. P. Pompa, L. Martiradonna, A. D. Torre, F. D. Sala, L. Manna, M. De Vittorio, F. Calabi, R. Cingolani, and R. Rinaldi, Nat. Nanotechnol. **1**, 126 (2006).
[11] P. Anger, P. Bharadwaj, and L. Novotny, Phys. Rev. Lett. **96**, 113002 (2006).
[12] C. Soennichsen and A. P. Alivisatos, Nano Lett. **5**, 301 (2005).
[13] N. Liu, M. Mesch, T. Weiss, M. Hentschel, and H. Giessen, Nano Lett. **10**, 2342 (2010).
[14] J. N. Anker, W. P. Hall, O. Lyandres, N. C. Shah, J. Zhao, and R. P. Van Duyne, Nat. Mater. **7**, 442 (2008).
[15] C. Wu, A. B. Khanikaev, R. Adato, N. Arju, A. A. Yanik, H. Altug, and G. Shvets, Nat. Mater. **11**, 69 (2011).
[16] U. Fano, Phys. Rev. **124**, 1866 (1961).
[17] S. Zhang, D. A. Genov, Y. Wang, M. Liu, and X. Zhang, Phys. Rev. Lett. **101**, 047401 (2008).
[18] B. Gallinet and O. J. F. Martin, Phys. Rev. B **83**, 235427 (2011).
[19] B. Luk'yanchuk, N. I. Zheludev, S. A. Maier, N. J. Halas, P. Nordlander, H. Giessen, and C. T. Chong, Nat. Mater. **9**, 707 (2010).
[20] F. Neubrech, A. Pucci, T. W. Cornelius, S. Karim, A. G. Etxarri, and J. Aizpurua, Phys. Rev. Lett. **101**, 157403 (2008).
[21] I. M. Pryce, K. Aydin, Y. A. Kelaita, R. M. Briggs, and H. A. Atwater, Nano Lett. **10**, 4222 (2010).
[22] V. Giannini, Y. Francescato, H. Amrania, C. C. Phillips, and S. A. Maier, Nano Lett. **11**, 2835 (2011).
[23] R. M. Roth, N. C. Panoiu, M. M. Adams, J. I. Dadap, and R. M. Osgood, Jr., Opt. Lett. **32**, 3414 (2007).
[24] P. G. Thompson, C. G. Biris, E. J. Osley, O. Gaathon, R. M. Osgood, N. C. Panoiu, and P. A. Warburton, Opt. Express **19**, 25 035 (2011).
[25] J. A. Hutchison, D. M. O'Carroll, T. Schwartz, C. Genet, and T. W. Ebbesen, Angew. Chem. **123**, 2133 (2011).
[26] DiffractMOD, RSoft Design Group. http://www.rsoftdesign.com.
[27] M. A. Ordal, R. J. Bell, R. W. Alexander, L. L. Long, and M. R. Querry, Appl. Opt. **24**, 4493 (1985).
[28] See Supplemental Material at http://link.aps.org/supplemental/10.1103/PhysRevLett.110.087402 for (1) measured and simulated reflection, transmission and absorption spectra of the uncoated aperture array; (2) a list of symbols used in the quantum mechanical model and a table containing their fitted values.